The roles of wedging and friction in the mechanics of dental occlusal contacts

Thomas R. Katona (Corresponding author)
  Purdue School of Engineering and Technology
  Department of Mechanical Engineering and Energy

  Department of Orthodontics and Oral Facial Genetics
  Indiana University School of Dentistry, IUPUI
  1121 W. Michigan Street
  Indianapolis, IN 46202-5186, USA
  tkatona@iu.edu
  ORCID: 0000-0001-9949-7237

George J. Eckert
   Department of Biostatistics
   Indiana University School of Medicine, IUPUI
   410 W. 10th Street
   Indianapolis, IN 46202-5186, USA
   geckert@iu.edu
   ORCID: 0000-0001-7798-7155

The roles of wedging and friction in the mechanics of dental occlusal contacts

ABSTRACT

Objective: The primary aim of this project is to elucidate the basic mechanical engineering principles that govern and explain unexpected and counter-intuitive occlusal contact force measurements.

Methods: Forces were measured on matched pairs of first molar denture, ceramic and stainless steel crowns during occlusion and disclusion, with human saliva and dry (control). The weighted maxillary assembly, guided by a precision slide, was lowered onto, and raised from, the mandibular crown. The forces experienced by the mandibular tooth were continuously measured by the load cell that supported it. Statistical analyses included LOESS smoothing splines and generalized additive models. Principles of basic statics and classic friction were applied to explain and validate the results.

Results: It was determined that within the span of a single chomp, the in-occlusal plane force component ($\mathbf{F_{lateral}}$) on the tooth is highly variable in direction and/or magnitude. The most salient observations were that $F_{lateral}$ was higher in disclusion than in occlusion, and the largest $F_{lateral}$ did not necessarily occur when the bite force was maximum. Furthermore, saliva significantly affected the results.

Conclusions: The results demonstrated that contacting teeth experience complex transient mechanical environments that can be readily explained with elementary engineering principles involving wedging and friction at the occlusal contacts.

1. Introduction

It is recognized that the mechanical environment of the masticatory system is complex, and that, despite a long history of research, it is still insufficiently elucidated (Rohrle, Saini, & Ackland, 2018). Moreover, some analytical (Katona, 2001, 2009) and experimental (Beninati & Katona, 2019; Mitchem, Katona, & Moser, 2017) studies, including this one, demonstrate that the mechanics of occlusal surface – occlusal surface contact, a key component in the system, is far more intricate than is commonly perceived. Largely non- or counter-intuitive, these findings are unlikely to be readily incorporated into mainstream clinical practice and experimental designs. Thus, a purpose of this paper is to explain and rigorously validate, with the application of elementary engineering principles, the perplexing findings about occlusal contact forces.

When cusped occlusal surfaces are brought together and then separated, as in **Fig. 1A**, wedging actions of the incline contacts produce a transient in-occlusal plane force component ($F_{lateral}$) on teeth and dental arches, **Figs. 1B** and **C** (Beninati & Katona, 2019; Mitchem et al., 2017). Thus, in the course of a single chomp (a complete occlusion-disclusion cycle), $F_{lateral}$, considered to be a periodontium-damaging occlusal load (Brune, Stiesch, Eisenburger, & Greuling, 2019; Dawson, 2006; Harrel & Nunn, 2009; Okeson, 2013; Passanezi & Sant'Ana, 2019; Yang & Chung, 2019) undergoes a wide range of magnitudes and directions. Furthermore, as the bite force changes, the contacts slide. This creates friction, and therefore, salivas also affect $F_{lateral}$ (McCrea, Katona, & Eckert, 2015). Thus, the quality and/or quantity of saliva could be a factor in occlusal trauma and TMD (Katona, 2001). In general, the continuously changing magnitude and direction of $F_{lateral}$ depend on the instantaneous bite force, occlusal anatomy, occlusal relationships, and crown materials (Beninati & Katona, 2019; Mitchem et al., 2017).

The non- or counter-intuitive experimental findings include that the maximum $F_{lateral}$ does not necessarily occur when the occlusal force is maximum, and that the relationship between the bite force and $F_{lateral}$ is different during occlusion than during disclusion. More unexpectedly, disclusion tends to produce larger magnitudes of $F_{lateral}$ (Katona & Eckert, 2017; Mitchem et al., 2017). It was also observed that flat-plane (0° cusp) stainless steel crowns can produce larger $F_{lateral}$ than 33° denture teeth (McCrea et al., 2015). Additionally, the general understanding of occlusal contact mechanics is muddled by the demonstration that the universally used occlusion detection products, *i.e.*, the traditional ribbons, and in particular, the state-of-the-art T-Scan system (Tekscan, South Boston, MA, USA), characterize artefactual occlusions that they themselves create by modifying direct crown-crown contacts into unique, product-specific, crown-product-crown interactions (Beninati & Katona, 2019; Helms, Katona, & Eckert, 2012; Mitchem et al., 2017).

Thus, the focus of this paper is on the elementary mechanical engineering principles that explain these perplexing, but important, nuances of occlusion biomechanics. The product testing aspects of the data, and a more detailed description of the methods, have already been published (McCrea et al., 2015).

2. Materials and Methods

The testing apparatus, **Fig. 1A**, consists of a ~15.3 N weighted (*i.e.*, the maximum bite force) upper assembly that is guided by a precision vertical slide (Mini-Guide, Double Carriage, Model #SEBS 9BUU2-195, Nippon Bearing Co, Ojiya, Japan) that supports the maxillary crown. The lower assembly is a load cell (Gamma Transducer, SI-65-5, ATI Industrial Automation, Apex, NC) that supports the mandibular crown and measures the 3 force components (F_x, F_y and F_z) 0 - 65 ± 0.0125 N.

Three pairs of opposing crowns were tested: Portrait IPN 33° left 1st molar denture teeth (Dentsply International, York, PA, USA), IPS Empress CAD esthetic ceramic crowns (Ivoclar

Vivadent, Schaan, Lichtenstein) and stainless steel crowns (3M ESPE, St. Paul, MN, USA), **Fig. 1A** inserts. The surfaces were dry (control) or wetted with human saliva (IRB approved bio bank #1105005588).

After the specimens were aligned in the apparatus, a testing machine (MTS Bionix 858, MTS Corp., Minneapolis, MN), in ramp displacement control mode (0.2 Hz, 4.0 mm amplitude), was used to lower/raise the weighted maxillary crown onto/from the mandibular crown while the forces acting on the latter, **Fig. 1B**, were continuously recorded by the load cell at 100 Hz. The saliva was applied to both occlusal surfaces, and after each run, the surfaces were cleaned with alcohol-soaked gauze and dried with a dry gauze and clinical quality compressed air.

Statistical analyses included LOESS smoothing splines and generalized additive models (GAM). LOESS splines used a span of 0.1 and 2nd degree polynomials. GAM used penalized thin-plate regression splines and were tested for significant differences between occlusion and disclusion and between human saliva and its dry control. A 5% significance level was used for all tests. Analyses were performed using the statistical software R (https://www.r-project.org/), via the GAM function from the MGCV package and the LOESS function.

3. Results
The curves in **Fig. 2** are the loci of all points during occlusion ($F_z = 0 \rightarrow 15$ N, solid lines) and disclusion ($F_z = 15 \rightarrow 0$ N, dashed lines) with human saliva (HS, thick lines) specimens and their dry controls (thin lines). As these are plots of F_y vs. F_x, an arrow drawn from the origin to any point on a curve is the **$F_{lateral}$** force vector associated with a specific F_z, **Fig. 1C**. As illustrations, all arrows indicated by the open circles (○) correspond to $F_z = 6$ N during occlusion (*i.e.*, when the bite force increased to 6 N) and disclusion (*i.e.*, when the bite force decreased to 6 N).

With the 6 N bite force, compared to control, HS has minimal effect on ceramic and SS. With ceramic, **$F_{lateral}$** in occlusion and disclusion are in the about same disto-buccal direction but the latter is ~70% larger, ~1.56 N vs. ~0.90 N. With SS, the disclusion vs. occlusion magnitude and direction differences are larger, ~2.70 N vs. ~1.32 N. With denture, **$F_{lateral}$** magnitudes are relatively uniform, however their directions are the most divergent.

The open square symbol (□) on the SS graph indicates the data point for $F_{lateral} = 1.28$ N in disclusion for control, similar in magnitude to the 1.29 N **$F_{lateral}$** vector (circle) also for control but in occlusion. The significance of this comparison is that the former and latter, although equal in magnitude, were produced by ($F_z =$) 2.9 N and 6.0 N bite forces, respectively. The contrast is more drastic with ceramic with HS in which the 6 N bite force in occlusion generated an $F_{lateral} = 0.89$ N (circle), but it took only a 0.5 N disclusion force to produce a nearly identical $F_{lateral} = 0.90$ N (open square). These are specific examples of the more general (counter-intuitive) observation that disclusion tends to generate larger **$F_{lateral}$** than occlusion. Also surprisingly, the largest forces are associated with the monoplane (0° cusp) SS crowns.

Figure 3 shows, as functions of bite force (F_z), the **$F_{lateral}$** magnitudes (left column) and the corresponding θ (right column) for denture (**A** and **B**), ceramic (**C** and **D**) and SS (**E** and **F**) during occlusion (solid lines) and disclusion (dashed lines). Thick and thin lines are the saliva and dry specimens, respectively. The HS vs. dry differences in $F_{lateral}$, θ, F_x and F_y curves were not statistically significant (p = 0.73 – 0.98) for ceramic in disclusion and for the F_y of denture in disclusion, p = 0.62. All other differences were significant (p < 0.0001) except $F_{lateral}$ in occlusion for denture, p = 0.0003. The occlusion vs. disclusion differences in $F_{lateral}$, θ, F_x and F_y were statistically significant (p < 0.001).

In **Fig. 4A**, all F_x and F_y force components acting on denture are plotted as functions of time, *i.e.*, sequentially, as acquired at the 0.01 second interval (100 Hz) data collection rate. Similarly, the results are shown for ceramic and SS in **Figs. 4B** and **C**, respectively.

The most salient overall observations about the measured transient forces are that:

- They are different in occlusion than in disclusion.
- They tend to be larger in disclusion than occlusion.
- Their largest magnitudes do not necessarily occur when the bite force (F_z) is maximum.

These overall results with 3 crown materials and human saliva replicate those of our earlier studies in which the effects of cusp angulations, occlusal relationships (*i.e.*, slight, ±0.05 mm, departures from Class I centric), the presence of various artificial salivas and articulating products (papers, films, silk, and T-Scan) were examined (Beninati & Katona, 2019; Helms et al., 2012; Katona & Eckert, 2017; McCrea et al., 2015; Mitchem et al., 2017).

A more in-depth inspection of **Fig. 3** reveals interesting behaviors.

- The 3 tooth pairs generate grossly different **$F_{lateral}$** magnitude (**A** vs. **C** vs. **E**) and θ (**B** vs. **D** vs. **F**) profiles, with or without saliva.
- Given the same bite force (F_z), disclusion (dashed lines) generally produces larger magnitudes of **$F_{lateral}$** than occlusion (solid lines), shown in **A**, **C** and **E**.
- When compared to the $F_{lateral} = F_z$ line (labelled in **A**), with small bite force,
  - $F_{lateral} \cong F_z$ in occlusion and disclusion (**A**) or
  - $F_{lateral} > F_z$ in disclusion (**C**) or
  - $F_{lateral} < F_z$ in occlusion and disclusion (**E**).
- **$F_{lateral}$** can decrease in magnitude as the bite force increases in occlusion (**A**), and it can increase as the bite force decreases in disclusion (**A** and **E**).
- The **$F_{lateral}$** occlusion/disclusion magnitude discrepancy with denture (**A**) is smaller than with the SS crowns (**E**), but the opposite is true about θ (**F** vs. **B**).
- The maximum magnitude of **$F_{lateral}$** does not necessarily coincide with the maximum magnitude of the bite force, **A** and **E**. With denture, the maximum $F_{lateral}$ occurs at F_z = ~2.9 N and ~6.5 N during occlusion and disclusion, respectively, **A**. The maximum $F_{lateral}$ takes place at F_z = ~9.3 N during the disclusion of SS, **E**.
- The monoplane occlusal surface (SS) generates the highest $F_{lateral}$.

4. Discussion

Direct occlusal surface – occlusal surface contacts are central to clinical conditions related to clenching, bruxism and wear facets. They are potential causes of enamel and restoration failures, dental pain, and likely contributors to temporomandibular disorders (TMD) and noncarious cervical lesions (NCCL). Occlusal detection products (paper, silk, and film) or T-Scan are ever-present clinical armamentaria for the assessment of these contacts. The emphasis in this paper is on the mechanics that explicate the above-presented, largely non- and counter-intuitive, contact results. Friction and wedging, fundamentals in elementary statics, serve as the mechanical engineering foundations.

The following should be considered:

- The occlusal anatomies of the 3 specimen pairs are different.
- The pairs are of different materials; thus the frictions are dissimilar, and therefore,
- differently affected by saliva.
- All pairs were arranged in Class I molar relationship, but that does not constitute precise or equivalent positioning.

Thus, the results reflect differences in occlusal anatomy, crown material, type of saliva, and relative crown positioning.

4.1. Force vector representations

The primary focus is on $F_{lateral}$, the force component that acts within the occlusal plane. Depending on application and convenience, vector entities such as $F_{lateral}$ can be depicted in several ways. Herein, we use vector arrows (**Figs. 1C** and **2**), magnitude with direction, θ (**Figs. 1C** and **3**), and F_x and F_y components (**Figs. 1C** and **4**). In these 3 representations, 2 vectors are equal, respectively, if their vector arrow depictions are the same length *and* point in the same direction, if their respective magnitudes *and* directions (θ) are equal, or if their respective $F_x = F_x$ *and* $F_y = F_y$. In addition, for 2 *force* vectors to be equal, their lines-of-action, or points-of-application, must be the same. (By convention, a bolded quantity such as "$F_{lateral}$" refers to the vector, whereas "$F_{lateral}$" is the magnitude of $F_{lateral}$.)

4.2. Contacts

When a pair of opposing crowns are brought into contact by a bite force, F_z, there is an instant in which a single occlusal contact force, F_1, occurs somewhere on the occlusal table, **Fig. 5A**. As the contact is likely on a cusp incline, F_1 is off-vertical, so it can be resolved into its horizontal (F_{1y}) and vertical (F_{1z}) components. The effect of F_{1y} (wedging) on the lower tooth is to produce a tendency for counter-clockwise (ccw) rotation and buccal translation, displacements indicated by the open arrowheads. And, according to Newton's 3rd Law, the same magnitude F_{1y}, but in the opposite direction (not shown), acts on the maxillary tooth. Thus, the tendency of the upper tooth is to rotate ccw and to translate palatally, as shown by the open arrowheads. Hence, as the occlusal force (F_z) is increased, in the instant shown in **Fig. 5B**, the displacement tendencies of both teeth are consistent with the formation of a second contact, F_2. (The F_z-components also produce potential tooth rotations, however their moment arms are generally much smaller than those of the F_y-components.) Thus, with the initial contact, the lateral force component, $F_{lateral}$ (= F_{1y}, in this 2-dimensional example) is toward the buccal, **Fig. 5A**. With the larger bite force, **Fig. 5B**, the net lateral force $F_{lateral}$ (= $F_{2y} - F_{1y}$) is smaller and it acts toward the lingual. With additional increases in F_z, the interactions become more intricate, as in the instant in **Fig. 5C**, with the formation of a third contact, F_3, that results in a larger $F_{lateral}$ toward the lingual. With the largest F_z, **Fig. 5D**, a contact is lost and $F_{lateral}$ disappears. Thus, this hypothetical scenario recreates the experimental observations that the largest magnitudes of $F_{lateral}$ do not necessarily occur when the bite force, F_z, is the largest, and that $F_{lateral}$ can decrease with increasing F_z.

Contrary to the notion that 0° cusps generate low lateral forces, it was noted that the monoplane SS crown produced the largest $F_{lateral}$, **Figs. 2** and **3**. If the contacting surfaces of 2 flat occlusal surfaces are not perpendicular to the applied force (F_z), there will be a lateral force, but unlike with multiple cusps, there is no possibility of an additional contact that could counter that lateral force. That is, in **Fig. 5**, with a flat-plane there could not be an F_2 nor an F_3.

The bite force (F_z) is distributed in an unknown proportion among an unknown number (n) of individual occlusal contact points. However, as illustrated in **Fig. 5**, at all times, the vertical force components of the n individual contacts must sum to F_z, *i.e.*, $F_z = F_{1z} + F_{2z} + F_{3z} + . . . + F_{nz}$. Similarly, $F_y = F_{1y} + F_{2y} + F_{3y} + . . . + F_{ny}$, and in the 3rd (mesio-distal) dimension, not shown, $F_x = F_{1x} + F_{2x} + F_{3x} + . . . + F_{nx}$. As the lower tooth is supported only by the load cell, the load cell must provide (and therefore, it can measure) F_z, F_y and F_x, the force components that maintain the lower tooth in equilibrium. Thus, the experimental design side-steps the individual unknown (and unmeasurable) occlusal contact force vectors.

There are 3 important points to keep in mind about the above described scenarios. First, the 2-dimmensional **Fig. 5** depictions are of contacts between buccal and lingual side inclines. These contacts generate the F_y force components shown in the diagrams. In 3-dimmensions, there are also contacts between mesial and distal slopes that produce the F_x components. And, there are contacts on cusp incline slopes that are not aligned with the mesial-distal / buccal-lingual (x-y) coordinate system. Those contacts, for example on cusp ridges, produce F_x *and* F_y

components. Thus, the 3-dimmensional occlusal contact patterns and the associated contact forces are extremely complex.

The second point is that, as explained above, the load cell measures the sums of the individually unknown occlusal contact force components. Thus, any alteration in the magnitude, direction and/or location of any individual occlusal contact force is reflected by changes in the load cell readings. And conversely, a change in load cell measurements can only occur if there is a change in at least one of the occlusal contacts.

The third point is that during occlusion and disclusion there is relative movement between cusps that causes the contacts (**Fig. 5**) to slide along their respective inclines, thus introducing friction (Brune et al., 2019; Katona, 2001; McCrea et al., 2015). The presence of friction explains, below, the occlusion/disclusion dichotomy.

4.3. Friction

The mechanics of the individual occlusal sliding contacts is akin to the classic statics friction problem of a block being pushed/pulled (occlusion/disclusion) along a surface, **Fig. 6**. Consider a block of weight W that can be pushed to the left or pulled to the right with, respectively, force F_L or F_R, applied to the pivoted (at B) handle, **Fig. 6A**. With F_L pushing to the left at A, **Fig. 6B** shows the solution for the forces acting on the free-body-diagram (FBD) of the handle. Horizontal force equilibrium dictates that there must be an F_L acting to the right at B. The 2 F_Ls, a couple, produce a counterclockwise moment, so for moment equilibrium, there must be vertical forces F_{VL} at A and B, as shown. Similarly, the FBD of the handle with F_R is depicted in **Fig. 6C**. Using the solution in **6B**, **Fig. 6D** is the FBD of the block. *N* is the normal (perpendicular) force applied by the surface to the block, which, by vertical force equilibrium is $N = W + F_{VL}$. The impending motion of the block is to the left, so the resisting force of friction, *f*, is drawn to the right. Furthermore, according to basic friction theory, with impending motion, $f = uN$, where µ is the coefficient of friction between block and surface. Thus, by horizontal equilibrium of the block, **Fig. 6D**, $F_L = f = uN = \mu(W + F_{VL})$ or $F_L = \mu(W + F_{VL})$, and therefore, $\mu W = F_L - \mu F_{VL}$. The same approach applied to **Figs. 6C** and **E** yields, $\mu W = F_R + \mu F_{VR}$. As µW = µW, it follows from the last 2 equations that, $F_L - \mu F_{VL} = F_R + \mu F_{VR}$, and therefore, $(F_L - F_R) = \mu F_{VL} + \mu F_{VR} = \mu(F_{VL} + F_{VR})$. As $\mu > 0$, $F_{VL} > 0$ and $F_{VR} > 0$, it must be that $\mu(F_{VL} + F_{VR}) > 0$. Hence, $(F_L - F_R) > 0$, and therefore, $F_L > F_R$. Thus, a larger force is required to push the block to the left (~occlusion) than to pull it to the right (~disclusion). Friction, therefore, explains the differences in the force environments associated with occlusion vs. disclusion.

This critical role of friction in the mechanical environment is confirmed by the statistically significant effects of saliva, which affects friction through its lubricative properties.

4.4. Relevance

In clinical and research contexts, a "bite force" is commonly considered as a force of constant, rather than transient, magnitude and/or direction. But the demonstrated transience during a single chomp impacts 2 types of problems. One involves the occlusal surface itself, for example, enamel and restoration wear and fracture. The 2nd is about the supporting structures (root, PDL, bone, implant-bone interactions, etc.). For the former, details about the individual contact forces are important because the phenomena in question occur at the contacts. For the latter, such contact detail is irrelevant because the issues arise at a distance from the contacts (Saint-Venant's principle). As this experimental approach combines the effects of the unquantifiable individual occlusal contact forces, the method is inapplicable to the first type (occlusal surface) problem other than to emphasize the inconstancy of the individual contact forces and their differences during occlusion vs. disclusion. The details of the individual contacts and the high variability of the forces ought to be taken into account in some prominent applications, discussed below. In all

instances, it is imperative to keep in mind that, as noted above, a force is a vector quantity, meaning that in the context of occlusion, force direction is just as important as its magnitude.

4.4.1 Occlusal contact marking products and T-Scan

Concerns about occlusion detection products (articulating papers, silk and film) have been extensively researched. The focus has been on the correlation between ink-mark characteristics (e.g., darkness and size) and the associated contact force magnitude, and the visual interpretation of those marks (Reddy, Kumar, & Grandhi, 2018). However, these products' inherent reliance on artefactual occlusions (Beninati & Katona, 2019; Mitchem, Katona, & Moser, 2018) has been mostly ignored. In the current context, there are other serious issues.

Consider the hypothetical situation, **Fig. 7A**, in which contact forces F_1, F_2 and F_3 act on the crown. Suppose that, based on ink marks, F_1, the strongest contact force, is deemed sufficiently hard to warrant adjustment. Based on its location on the cusp incline, the operator would observe, correctly, that that contact force has a large *buccal* component, F_{1y}. But, in fact, overall, the contact forces produce a relatively small *lingually* directed $F_{lateral}$ due to the combined lingual components of the 2 smaller contact forces. And because the adjustment would decrease F_{1y}, the result would be an undesirable increase in $F_{lateral}$ towards the lingual. The amount of change in $F_{lateral}$ is unpredictable because the F_1 modification would also produce concomitant changes in F_2 and F_3. Also, note that in 3 dimensions (vs. the 2-dimension discussions), in addition to the bucco-lingual force components, the mesio-distal components would also be involved.

Contact forces are associated with contacting surfaces with specific orientations. (The direction of a surface is defined by the direction of the perpendicular, or normal, vector to the plane.) The orientations of the contacting surfaces, coupled with the effects of friction, are the determinants of contact force direction.

These specific issues are not directly relevant to the T-Scan system because, egregiously, it simply ignores the critical in-occlusal plane components of the contact forces.

4.4.2 Wear facets

Wear facets have been used for the indirect assessment of occlusal forces (Benazzi, Kullmer, Grosse, & Weber, 2011) in experimental and clinical applications. The simple scenario diagrammed in **Fig. 7A** illustrates the pitfalls in using wear facets for such purposes. In this hypothetical situation, F_1, the largest of the contact forces, is most likely to produce a wear facet. Based on its location, it would be concluded that the tooth experienced a large buccally directed occlusal force component, F_{1y}. The smaller forces, F_2 and F_3, are less likely to create facets, however, as discussed above (4.4.1), their combined action ($F_{2y} + F_{3y}$) is a horizontal force toward the lingual that is larger than the buccal component of F_1. Hence, the actual net overall $F_{lateral}$ is directed toward the lingual, which is diametrically opposite to the erroneous wear facet–based inference. Thus, wear facets are unreliable indicators of the overall mechanical environment of the tooth.

4.4.3 Axial loading

According to cornerstone clinical dogma, occlusal forces should be directed along the long-axes of teeth to minimize the potential for periodontal damage (Dawson, 2006; Okeson, 2013). Such loading can be mathematically defined by $F_{lateral} = 0$. As $F_{lateral}$ is shown to be transient in magnitude and/or direction, **Fig. 2**, the $F_{lateral} = 0$ condition is, at best, ephemeral. Aside from that, anatomic configurations that are simultaneously consistent with static equilibrium and $F_{lateral} = 0$ on both opposing teeth are, essentially, impossible (Katona, 2009).

4.4.4 Non-carious cervical lesions (NCCLs)

The role of the mechanical environment in the etiology of NCCLs is an ongoing controversy (Senna, Del Bel Cury, & Rosing, 2012; Silva et al., 2013; Soares & Grippo, 2017; Telles, Pegoraro, & Pereira, 2006). The mechanical culprit is generally assumed to be damage caused by a bending of the tooth. But, as demonstrated, teeth experience a wide range of force magnitudes and directions during each chomp, which in turn, produces a wide range of bending moment magnitudes and directions. Thus, the initiation and/or propagation of NCCLs could result from load combination(s) during each chomp, not necessarily forces in a single specific direction.

4.4.5 Bite force sensors

Studies that involve subjects biting onto force sensors should be interpreted with great caution. Occlusal contact interactions of the sort depicted in **Fig. 5** produce the complex mechanical environments best illustrated in **Fig. 2**. It has been shown (Helms et al., 2012; Mitchem et al., 2017) that these environments are significantly altered by the presence of even relatively thin and compliant articulating paper, silk and film products, and much more so by the stiffer T-Scan sensor. In effect, rigid force sensors completely obliterate the occlusal anatomy, **Fig. 7B**, thus making it impossible for their measurements to bear any semblance to the physiological forces, **Fig. 7A**.

Thus, the major issues involving the above applications are:
- The unavailability of sufficient contact force vector information (direction, magnitude and line-of-action).
- The modification of contacts by occlusal indicator products resulting in artefactual contact forces.
- The inattention to the transience of force vectors during individual chomps.
- The extrapolation of an individual contact force to the load system on the tooth.

5. Conclusion

Despite its central role in a broad range of dental functions, the complexity of dental contact physics is generally overlooked. As demonstrated, the intricate contact interactions can be explained with 2 basic engineering concepts. The occlusion/disclusion differences are attributed to the effects of friction at the contacts. The unpredictable relationships between bite force and contact forces are caused by wedging while individual occlusal contacts are made and broken.

Disclosures

References

Benazzi, S., Kullmer, O., Grosse, I. R., & Weber, G. W. (2011). Using occlusal wear information and finite element analysis to investigate stress distributions in human molars. *J Anat, 219*(3), 259-272. doi:10.1111/j.1469-7580.2011.01396.x

Beninati, C. J., & Katona, T. R. (2019). The combined effects of salivas and occlusal indicators on occlusal contact forces. *J Oral Rehabil*. doi:10.1111/joor.12772

Brune, A., Stiesch, M., Eisenburger, M., & Greuling, A. (2019). The effect of different occlusal contact situations on peri-implant bone stress - A contact finite element analysis of indirect axial loading. *Mater Sci Eng C Mater Biol Appl, 99*, 367-373. doi:10.1016/j.msec.2019.01.104

Dawson, P. E. (2006). *Functional occlusion: from TMJ to smile design*. St. Louis, Mo: Mosby.

Harrel, S. K., & Nunn, M. E. (2009). The association of occlusal contacts with the presence of increased periodontal probing depth. *J Clin Periodontol, 36*(12), 1035-1042. doi:10.1111/j.1600-051X.2009.01486.x

Helms, R. B., Katona, T. R., & Eckert, G. J. (2012). Do occlusal contact detection products alter the occlusion? *J Oral Rehabil, 39*(5), 357-363. doi:10.1111/j.1365-2842.2011.02277.x

Katona, T. R. (2001). A mathematical analysis of the role of friction in occlusal trauma. *J Prosthet Dent, 86*(6), 636-643. doi:10.1067/mpr.2001.120068

Katona, T. R. (2009). An engineering analysis of dental occlusion principles. *Am J Orthod Dentofacial Orthop, 135*(6), 696 e691-698; discussion 696-697. doi:10.1016/j.ajodo.2008.04.020

Katona, T. R., & Eckert, G. J. (2017). The mechanics of dental occlusion and disclusion. *Clin Biomech (Bristol, Avon), 50*, 84-91. doi:10.1016/j.clinbiomech.2017.10.009

McCrea, E. S., Katona, T. R., & Eckert, G. J. (2015). The effects of salivas on occlusal forces. *J Oral Rehabil, 42*(5), 348-354. doi:10.1111/joor.12260

Mitchem, J. A., Katona, T. R., & Moser, E. A. S. (2017). Does the presence of an occlusal indicator product affect the contact forces between full dentitions? *J Oral Rehabil, 44*(10), 791-799. doi:10.1111/joor.12543

Mitchem, J. A., Katona, T. R., & Moser, E. A. S. (2018). Response to letter to the editor: "Does the presence of an occlusal indicator product affect the contact forces between full dentitions?". *J Oral Rehabil, 45*(7), 574. doi:10.1111/joor.12652

Okeson, J. P. (2013). *Management of temporomandibular disorders and occlusion* (7 ed.). St. Louis, Mo: Elsevier Mosby.

Passanezi, E., & Sant'Ana, A. C. P. (2019). Role of occlusion in periodontal disease. *Periodontol 2000, 79*(1), 129-150. doi:10.1111/prd.12251

Reddy, S., Kumar, P. S., & Grandhi, V. V. (2018). Relationship Between the Applied Occlusal Load and the Size of Markings Produced Due to Occlusal Contact Using Dental Articulating Paper and T-Scan: Comparative Study. *JMIR Biomed Eng, 3*(1), e11347. doi:10.2196/11347

Rohrle, O., Saini, H., & Ackland, D. C. (2018). Occlusal loading during biting from an experimental and simulation point of view. *Dent Mater, 34*(1), 58-68. doi:10.1016/j.dental.2017.09.005

Senna, P., Del Bel Cury, A., & Rosing, C. (2012). Non-carious cervical lesions and occlusion: a systematic review of clinical studies. *J Oral Rehabil, 39*(6), 450-462. doi:10.1111/j.1365-2842.2012.02290.x

Silva, A. G., Martins, C. C., Zina, L. G., Moreira, A. N., Paiva, S. M., Pordeus, I. A., & Magalhaes, C. S. (2013). The association between occlusal factors and noncarious cervical lesions: a systematic review. *J Dent, 41*(1), 9-16. doi:10.1016/j.jdent.2012.10.018

Soares, P., & Grippo, J. (2017). Noncarious Cervical Lesions and Cervical Dentin Hypersensitivity: Etiology. *Diagnosis, and Treatment: Quintessence Pub Co*.

Telles, D., Pegoraro, L. F., & Pereira, J. C. (2006). Incidence of noncarious cervical lesions and their relation to the presence of wear facets. *J Esthet Restor Dent, 18*(4), 178-183; discussion 184. doi:10.1111/j.1708-8240.2006.00015.x

Yang, S.-M., & Chung, H.-J. (2019). Three-dimentional finite element analysis of a mandibular premolar with reduced periodontal support under a non-axial load. *Oral Biology Research, 43*, 313-326. doi:10.21851/obr.43.04.201912.313
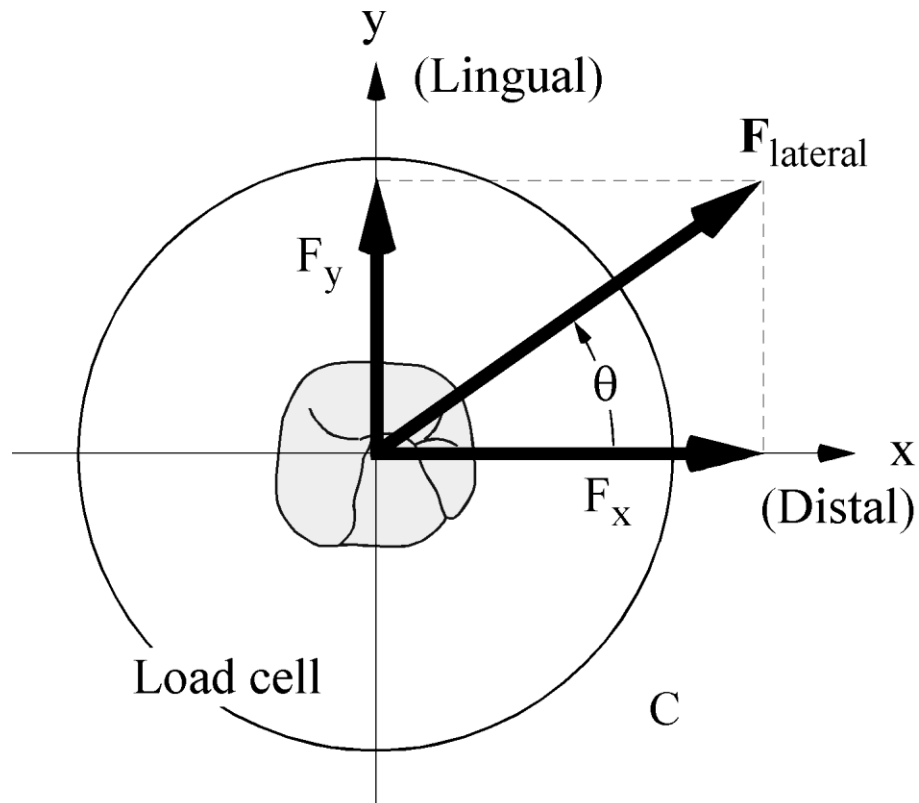
1A
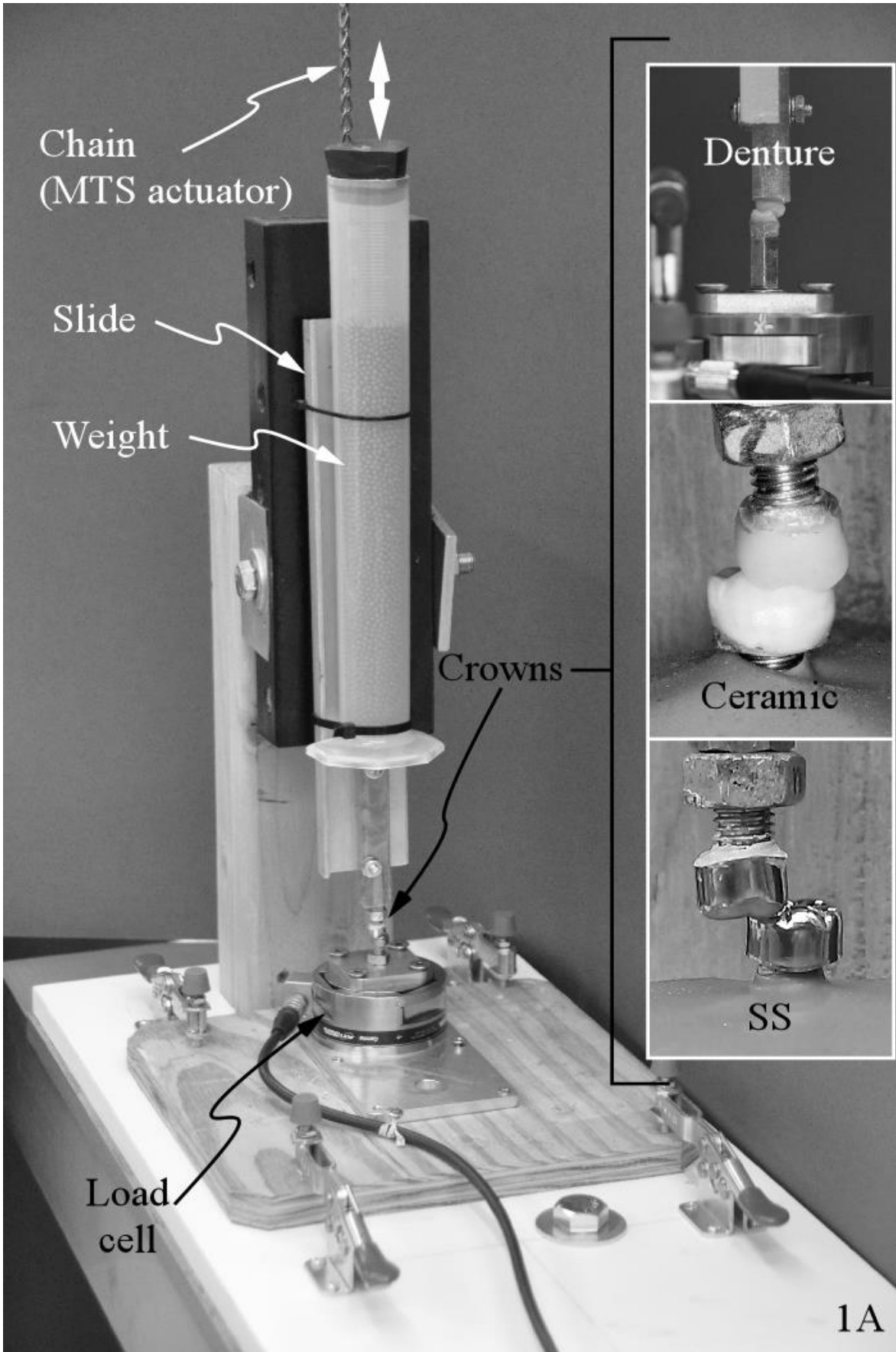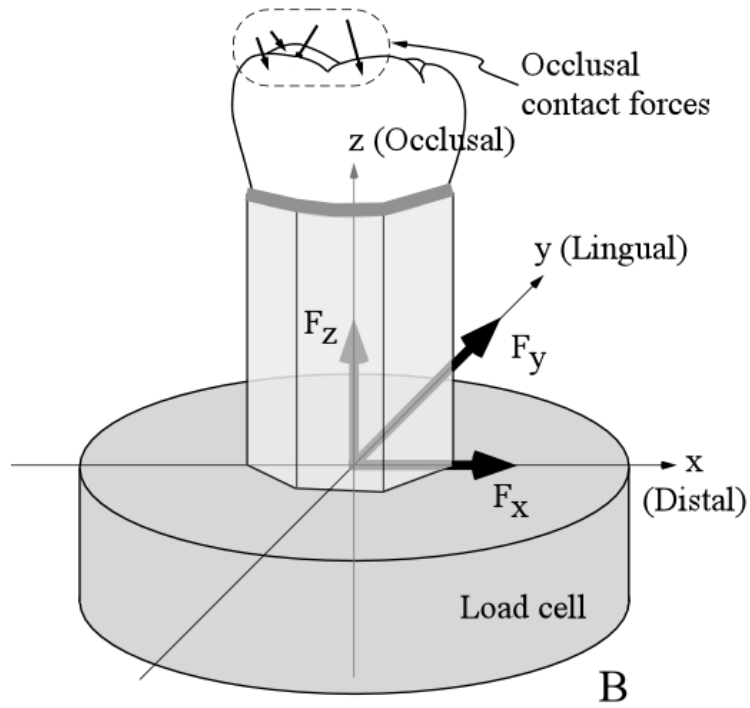
Fig. 1: (**A**) Testing apparatus. Inserts show denture, ceramic and SS specimens in various occlusal relationships. Molar Class I centric data are presented. (**B**) The 3 force components measured by the load cell. (**C**) Occlusal view of lower assembly. The in-occlusal plane force component magnitude ($F_{lateral}$) and its direction (θ) are derived from the load cell measured F_x and F_y as follows: $F_{lateral} = \sqrt{(F_x)^2 + (F_y)^2}$ (Pythagorean Theorem) and $\theta = \tan^{-1}\left[\frac{F_y}{F_x}\right]$.
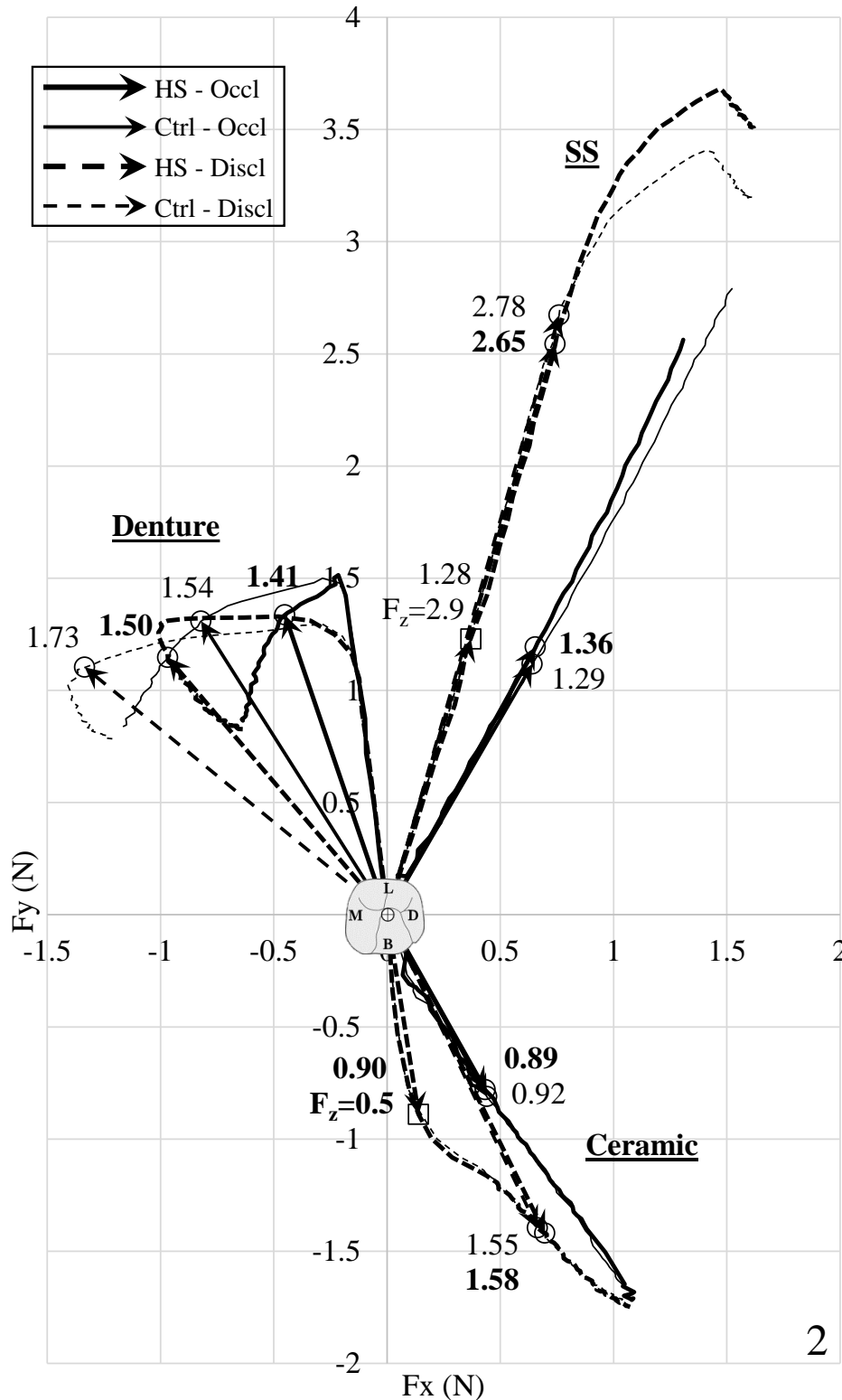
Fig. 2: **F**lateral results displayed as force vector arrows, F_y (N) vs. F_x (N). Solid and dashed lines represent occlusion ($F_z = 0 \rightarrow 15$ N) and disclusion ($F_z = 15 \rightarrow 0$ N), respectively. Thick and thin lines denote, respectively, saliva and its control. All circled arrowheads correspond to the bite force, $F_z = 6$ N, and the numbers at each arrow tip are the vector lengths, *i.e.*, the **F**lateral magnitudes. The curves represent the loci of points depicting the complete set of data points for occlusion (solid curves) and disclusion (dashed lines).
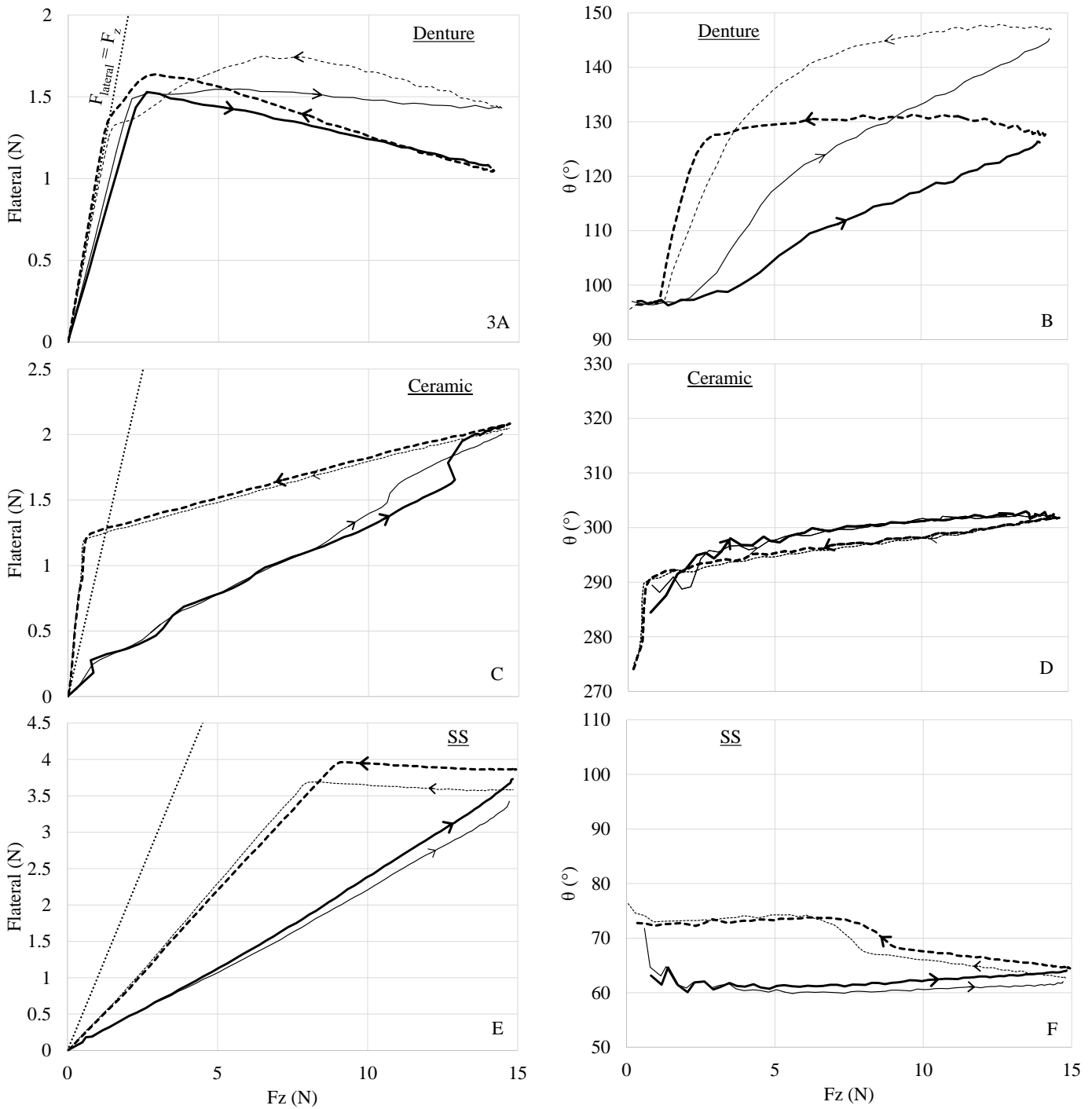
Fig. 3: Graphs of all $F_{lateral}$ (N) vs. F_z (N; bite force) and corresponding θ (°) vs. F_z, respectively, for (**A**, **B**) denture, (**C**, **D**) ceramic and (**E**, **F**) SS crowns with saliva (thick line) and its control (dry; thin line). In all graphs, occlusion ($F_z = 0 \rightarrow \sim 15$ N) and disclusion ($F_z = \sim 15 \rightarrow 0$ N) are represented by solid and dashed lines, respectively.
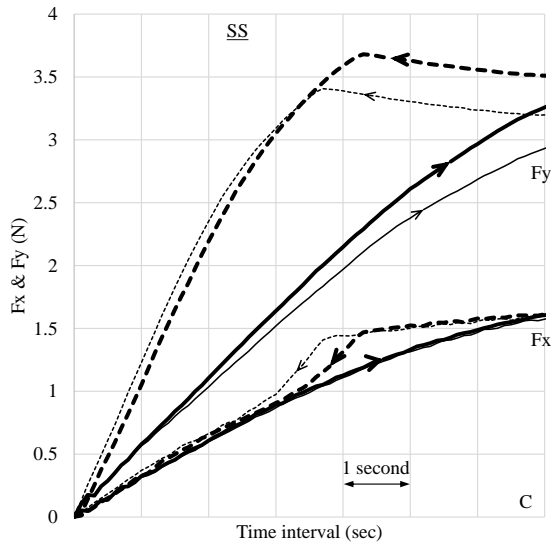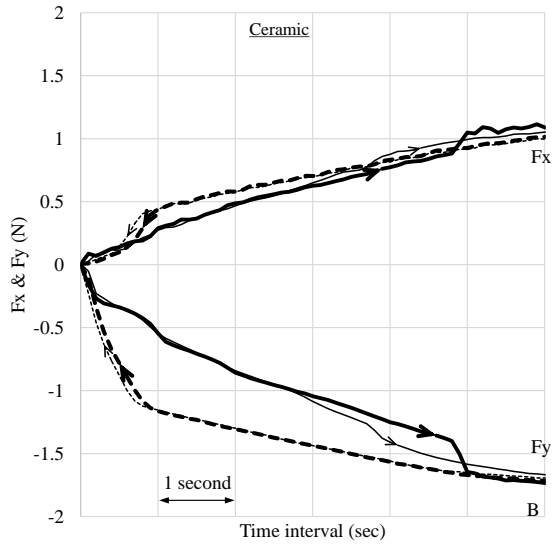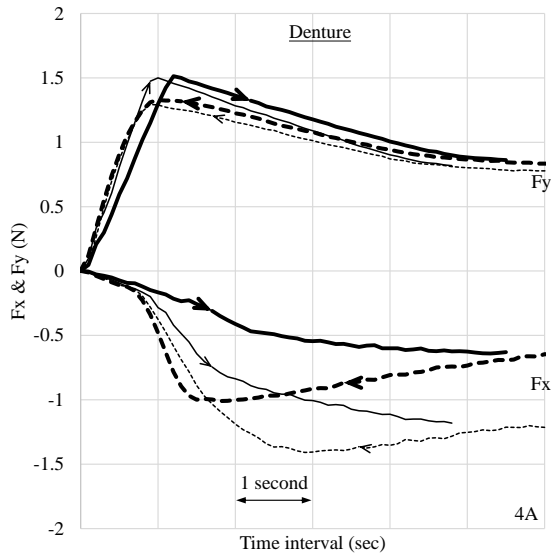
Fig. 4: F_x and F_y graphed in the sequence of acquisition, 100 data points/second. Line qualities are as in **Fig. 3**. (**A**) denture, (**B**) ceramic and (**C**) SS.
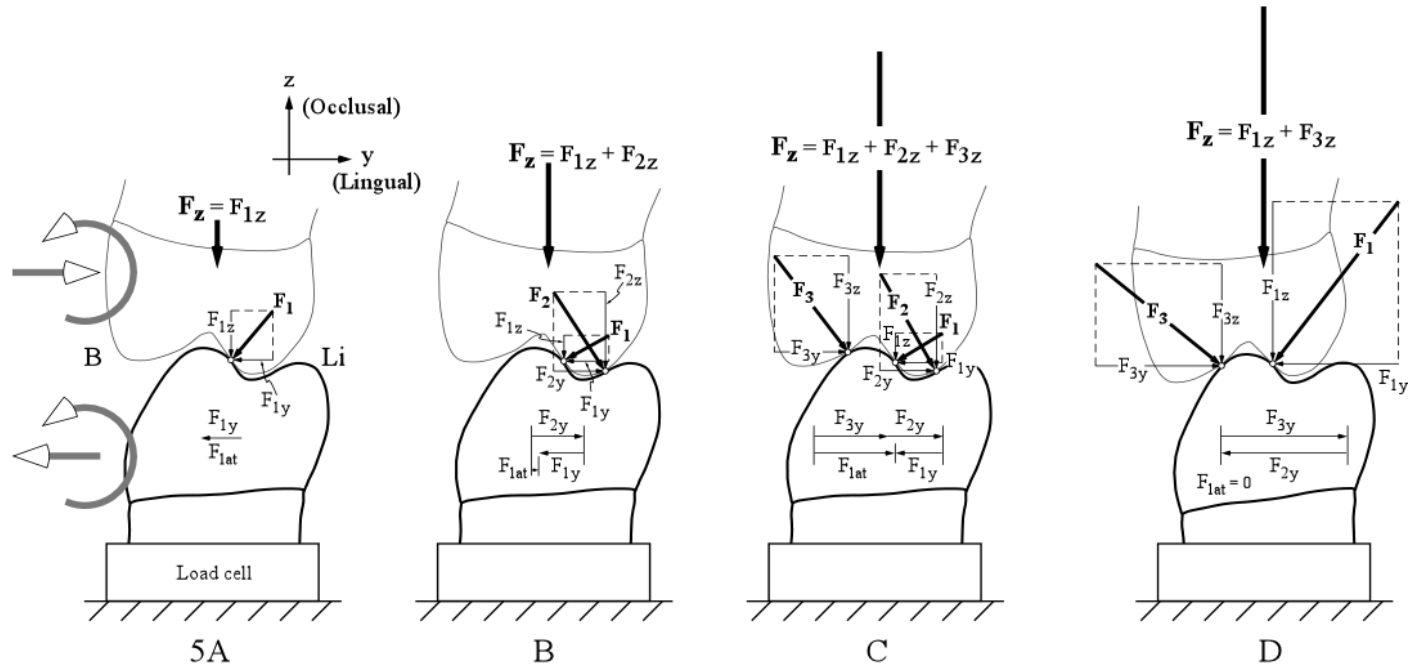
Fig. 5: Schematics of hypothetical occlusal contacts in 2 dimensions showing increasing, (**A**) → (**D**), bite force, F_z, applied onto the lower tooth. Forces F_1, F_2 and F_3 are the hypothetical individual occlusal contact forces acting on the lower tooth. Note that the sum of the vertical components of the individual contact forces ($F_{1z} + F_{2z} + F_{3z}$) must add-up to the applied force (F_z), while the bucco-lingual force (F_{lat}) on the lower tooth is the sum of the bucco-lingual (y) components of the individual contact forces ($F_{1y} + F_{2y} + F_{3y}$). Similar considerations, not shown, apply in the perpendicular (x) mesio-distal direction. Also note that F_1 in (**A**) is different in magnitude, direction and/or point of application from F_1 in (**B**), which in turn, is different from F_1 in (**C**), and so on. Similarly for F_2 and F_3. The open arrowheads indicate tooth displacements.
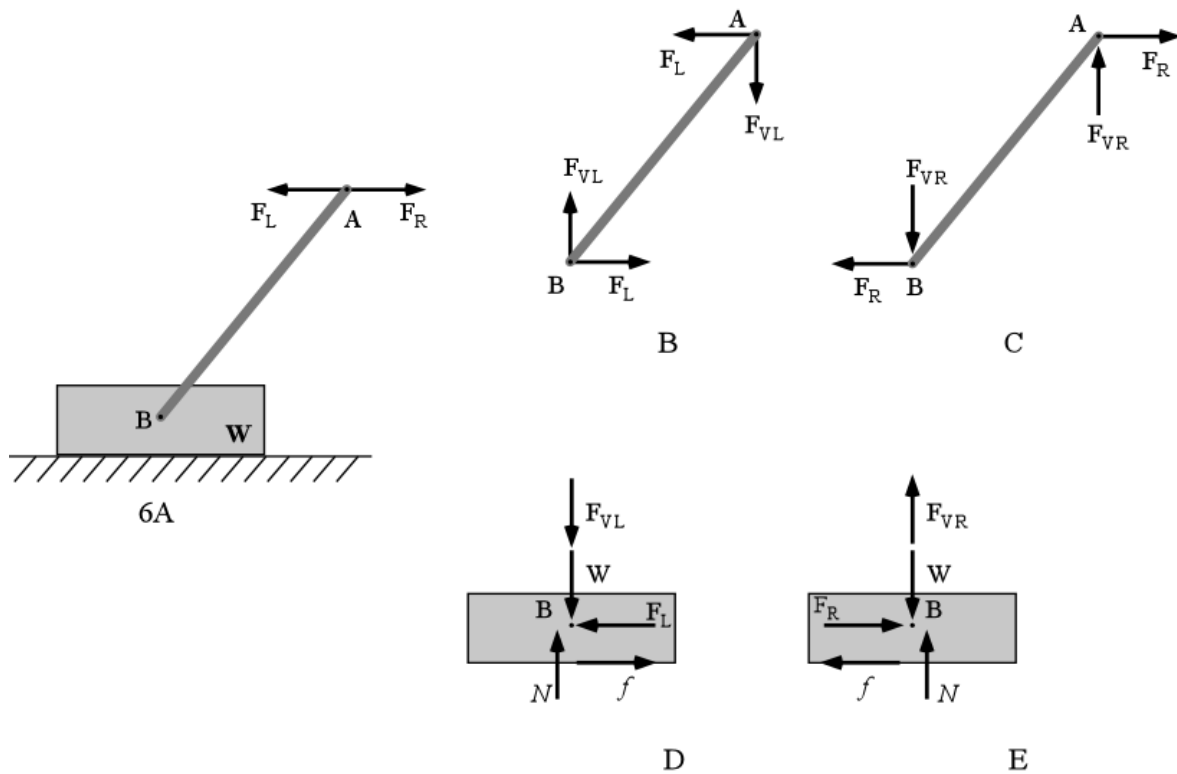
Fig. 6: Analogy for occlusion vs. disclusion. (**A**) A block of weight W can be pushed to the left (~occlusion) with force F_L or pulled to the right (~disclusion) with F_R. (**B**) The solution for the equilibrium forces acting on the handle with F_L applied at A. (**C**) as in (**B**) but for F_R. (**D**) With the solution in (**B**), this is the FBD of the block in which N is the normal (perpendicular) force applied by the surface to the block and f is the force of friction between surface and block. (**E**) as in (**D**) but for F_R. (Note that the effective weight of the block is increased in **D** (by F_{VL}) but decreased in E (by F_{VR}). Thus, seemingly, a heavier weight is moved to the left than to the right.)
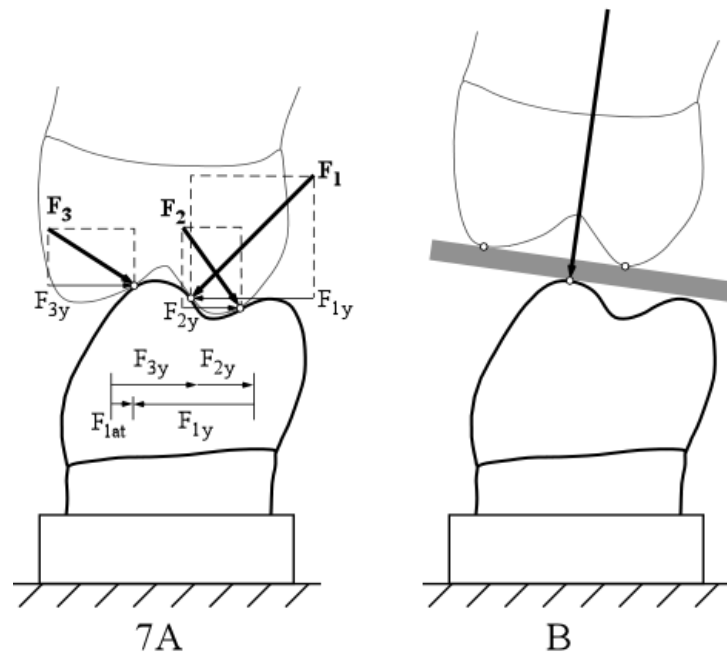
Fig. 7: (**A**) A hypothetical occlusal configuration. (**B**) The same occlusion with a rigid force transducer.